Stable Free Radicals Produced in Acrylate and Methacrylate Free Radical Polymerization: Comparative EPR Studies of Structure and the Effects of Cross-Linking

ARTICLE *in* MACROMOLECULES · FEBRUARY 1996

Impact Factor: 5.8 · DOI: 10.1021/ma951444w

2 AUTHORS, INCLUDING:

Randy Mehlenbacher
Army Research Laboratory
5 PUBLICATIONS **46** CITATIONS

SEE PROFILE

Stable Free Radicals Produced in Acrylate and Methacrylate Free Radical Polymerization: Comparative EPR Studies of Structure and the Effects of Cross-Linking

D. C. Doetschman* and R. C. Mehlenbacher†

Department of Chemistry, The State University of New York, Binghamton, New York 13902-6016

Douglas Cywar

Cytec Industries, 1937 West Main Street, P.O. Box 60, Stamford, Connecticut 06904-0060

Received September 26, 1995; Revised Manuscript Received December 8, 1995[⊗]

ABSTRACT: Electron paramagnetic resonance (EPR) examinations of the stable free radicals from the polymerizations of a series of monofunctional, difunctional, and trifunctional acrylates and methacrylates have been made. The continuous-wave (CW) EPR of polymers from selectively deuterated monofunctional monomers and the pulsed EPR of the nondeuterated polymers were also examined. The aim of the experiments was to attempt to clarify several points of disagreement concerning the identity and assignment of polymer free radicals. The EPR results on the polymethacrylates are in general agreement with past results and interpretations, in which isotropic hyperfine interactions are assigned to the methyl and methylene protons β to the central carbon of the propagating polymer radical. The rate of propagation of the observed radicals has been arrested by the high viscosity achieved in the polymer. The CW EPR spectra of the polyacrylates are well-simulated with two different models. In one model, the spectra are assigned to the propagating free radical with isotropic β-methylene proton interactions and an anisotropic α-proton coupling. In the other model, it is assumed that the secondary propagating radical abstracts a hydrogen from the polymer chain to form a tertiary radical flanked by two isotropically coupled methylene groups. The latter model gives a slightly better fit to the data. One of the unresolved problems with the EPR spectra of acrylate and methacrylate polymers has been the absence or selective broadening of certain expected hyperfine lines. One hypothesis is a dynamic polymer motion that exchanges methylene proton positions, resulting in an alternating homogeneous line width [Sakai, Y.; Iwasaki, M. *J. Polym. Sci. A-1* **1969**, *7*, 1719]. The spin−spin relaxation times, T_2, measured with pulsed EPR fail to support this hypothesis. We show that a static orientation distribution of the methylene protons with respect to the axis of the orbital of the odd electron [Best, M. E.; Kasai, P. H. *Macromolecules* **1989**, *22*, 2622] successfully leads to an alternating heterogeneous line width.

Introduction

The existence of unusually long-lived radicals in polymeric matrices is well-known.[1,2] In particular, photopolymerization of (meth)acrylic monomers yields samples with trapped radicals that can be readily detected by electron paramagnetic resonance (EPR).[1,2] The EPR signal intensities grow with monomer conversion as the rigidity of the environment increases. This effect is pronounced for the case of multifunctional (meth)acrylates wherein a cross-linked network is formed. The structure of the radicals has been the subject of many investigations. There is still no consensus on the conformation of the free radicals. Some disagreements persist even on the free radical chemical structures.

The structure and chemistry of the trapped radicals are relevant topics with regard to industrial applications of photopolymers,[3] since their fate may well influence final material properties.[4] In the case of "dry-film" photoresists based on multifunctional (meth)acrylates, which are widely used in the fabrication of printed circuit boards,[3] it is well-known that the time between ultraviolet (UV) exposure and development of the photoresist can influence manufacturing process parameters and final film properties.[5] It is likely that trapped radicals play a key role during this "hold time". The rates of free radical polymerization and cross-linking are highly sensitive functions of viscosity. Therefore, the resultant polymer properties can be controlled by the duration and conditions, such as temperature, imposed during the hold time. The work presented in this paper grew out of free radical structural questions raised during the course of an EPR study of hold-time conditions.

It has been generally accepted that the appearance of the free radical spectrum observed in the course of free radical methacrylate polymerizations is from the propagator radical. It is thought that these radicals achieve sufficient concentrations to be observed in the later stages of a roughly three-stage polymerization process.[6,7] First, when little or no polymerization has taken place and the viscosity is low, the mobility of the propagating free radicals favors bimolecular termination processes (predominantly disproportionation). These termination processes ordinarily keep propagating free radical concentrations low and undetectable. A second, intermediate stage ensues in which increased polymerization leads to mobility decreases, viscosity increases, and consequent slowing of the termination rates. At this stage the propagating free radical concentration becomes detectable. A final stage is usually observed in which further increases in radical concentration occur with diminishing rates. This presumably takes place because polymerization has become so extensive and molecular mobility is so low that initiation and propagation are also being inhibited.

Early workers found that detectable quantities of free radicals could be achieved in free radical methacrylate

† Present address: Louisiana School for Mathematics, Science and the Arts, 715 College Avenue, Natchitoches, LA 71457-3915.

[⊗] Abstract published in *Advance ACS Abstracts,* February 1, 1996.

0024-9297/96/2229-1807$12.00/0

polymerizations by precipitation of the polymer from (solution in) monomer or by the addition of a cross-linking agent such as a difunctional methacrylate.[1,2,7] These former studies, as well as γ-irradiation studies, gave a complex spectrum of five main lines with additional features from methacrylate or methacrylic acid samples. A three-line spectrum was observed from the acrylate or acrylic acid samples. All spectra were assigned to the propagating free radical.[8−10] A variety of explanations of these spectra, especially focusing on the methacrylate or methacrylic acid polymerizations, involve different rotational configurations of the polymer end group radical[8,11] or a dynamic equilibrium between the configurations.[12] The latter has been widely accepted, invoking a dynamic equilibrium between two conformations of the two $C_\beta-H$ bonds, which make projections of 55° and 65° on the normal to the $C_\alpha-C_\beta$ bond with respect to the axis of the p-orbital of the unpaired electron.[12] However, there has been a recent report from a study of a difunctional acrylate that there is a broad spectrum underlying the well-known three-line spectrum.[13] The broad spectrum has an integrated intensity of about twice that of the three-line spectrum.[13]

Most models assume that the EPR spectra of polymer radicals display an isotropic hyperfine structure without any anisotropic electron−nuclear dipolar interactions. This assumption is made even at low temperatures where the rates of radical tumbling might be expected to become too slow to average out the dipolar interactions. To our knowledge this assumption has not been put to a critical test, probably because of the complexities of the polymer systems and the computational simplicity of the isotropy assumption. In a wide variety of studies of methacrylic acid and methacrylate polymers, the β-methylene proton hyperfine coupling constants of the spectrum assigned to the propagating radical have been found to be in the ranges of 13−15 and 7.5−11 G.[12,14−16] These same studies found a coupling constant of 21.5−22.4 G for the β-methyl group proton hyperfine coupling constant. Coincidentally, the sum of the β-methylene proton coupling constants is approximately equal to the methyl coupling constant. If the dynamic model described previously for the β-methylene protons is assumed, this situation results in a spectrum with alternating line widths with five sharp lines and four interspersed broader lines.[12] In principle, the dynamically broadened four-line spectrum can be further resolved into eight separate lines in the limit of slow methylene proton site interchange. Sakai and Iwasaki present evidence for this eight-line spectrum between −5 °C and −30 °C in methacrylic acid polymer.[12] We are unaware of any work showing a similar dynamic β-methylene proton interchange in the radical in acrylic acid and acrylate polymers that results in an alternating line width. Such a result would be reasonable, since α-proton hyperfine interactions in secondary hydrocarbon, carbon-centered radicals are also on the order of 21−22 G. However, this situation may be complicated by the relatively larger anisotropic hyperfine coupling of the α-proton relative to the isotropic coupling in acrylic acid and acrylate polymers.[17]

The preceding considerations for the radical in the acrylate polymers assume that the long-lived radical is the propagator radical I. Recently, it has been suggested by Liang et al.[18,19] that the acrylate polymerization terminates with the abstraction of a midchain

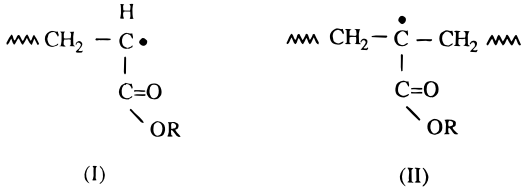

(I) (II)

hydrogen by the propagating secondary free radical I. The resulting radical product is a tertiary, midchain free radical II. Kloosterboer et al.[4] provide compelling chemical evidence from the EPR spectrum of the polymer from an α-deuterated acrylate monomer that structure I is not the structure of the radical. They found that the EPR spectrum is independent of α-deuteration. Best and Kasai[20] simulate the EPR spectra of the several local polymer conformations that might lead to radical II. They show that mainly the relatively unstable *gauche,gauche* precursor conformation is consistent with the observed EPR spectrum. Best and Kasai[20] also introduce a Gaussian distribution of the projections of the methylene protons with respect to the axis of the orbital of the odd electron. They did not perform a minimization to refine the parameters of their structural model, nor did they show that the results of their simulation with structure II were superior to a simulation of the spectrum with structure I. A recent continuous-flow EPR study of the polymerization of acrylic acid and related compounds with electrophilic radical initiators has been performed by Gilbert et al.[21] The study reveals the formation of midchain radicals at competitive rates in the tetrameric propagator radical and higher radical oligomers, which is suggestive of a 1,5-hydrogen shift mechanism.[21]

The Bloch equations have been solved for the dynamic model, insofar as they affect the pairs of lines making up the broad four-line part of the spectrum of the propagator-type radical in methacrylic acids, methacrylates, or their polymers.[12] According to the fits to experimental data, the pairs of lines became fully resolved when the average lifetime of a given configuration was 3.8×10^{-7} s or longer. Below an average configurational lifetime of 1.1×10^{-8} s, the pairs of lines were no longer resolvable. This was in approximate agreement with theory for the observed line pair separation of 6.9 G. Sakai and Iwasaki observed an unusual, increasing configurational lifetime with increasing temperature because the particular crystalline system of methacrylic acid was undergoing a phase transition.[12] However, normal temperature dependencies have been observed for related radicals in barium methacrylate[15] and alanine.[17]

Pulsed EPR methods, which are ideally suited for investigations of the dynamics of spin systems, have not yet been applied extensively to the dynamics of polymer systems. To our knowledge, only one such pulsed EPR study has been done, in which the microwave saturation recovery spectra of the radicals in γ-irradiated poly(methyl methacrylate) were recorded.[22] The method enabled the authors to discriminate between spectra from different radicals on the basis of their spin−lattice relaxation times, T_1. The dynamic interchange of the two β-methylene proton sites in the propagator or midchain radical would be expected to influence the spin−spin relaxation time, T_2, of the broad parts of the spectra. For example, in the spectrum analyzed by Sakai and Iwasaki,[12] one might expect T_2 to be approximately equal to the configuration lifetime, in the long lifetime limit. Thus, their dynamic model would

predict T_2 to be 400 ns or greater when the pairs of lines are well-resolved and on the order of 10 ns when the dynamically broadened pairs of lines are no longer resolvable.

We performed CW and pulsed EPR experiments addressing some of these questions about the chemical structure, conformation, and dynamic motions of the free radicals in acrylate and methacrylate polymers. A series of monofunctional, difunctional, and trifunctional monomers of both the acrylate and methacrylate types were examined to observe the dependence on polymer cross-linking. Room temperature CW EPR spectra of the free radicals in each type of polymer were least-squares-fitted by several models. Two models were of the type introduced by Sakai and Iwasaki.[12] Angular distribution models of the type introduced by Best and Kasai[20] for the propagator-type radical were fitted to the acrylate and methacrylate spectra. The acrylate spectra were also fit by a Best−Kasai angular distribution model for the midchain-type radical. Pulsed EPR measurements of the echo decay of the spectra were performed to examine the dynamic motions of the polymer proposed by Sakai and Iwasaki.[12]

Experimental Section

Polymerizations of methyl acrylate (MA), methyl methacrylate (MMA), 1,6-hexanediol diacrylate (HDA), ethylene glycol dimethacrylate (EGDMA), trimethylolpropane triacrylate (TMPTA), and trimethylolpropane trimethacrylate (TMPTMA), all from Aldrich Chemical Co., were examined. Polymerizations of methyl methacrylate deuterated at the methylene groups [MMA-d_2 or $D_2C{=}C(CH_3)COOCH_3$] or at the olefinic methyl groups [MMA-d_3 or $H_2C{=}C(CD_3)COOCH_3$], obtained from MSD Isotopes, were also examined. Inhibitor was removed from each protonated monomer by passage through columns prepared for inhibitor removal (Scientific Polymer Products, DHR-4). Deuterated monomers were passed over a column of beads removed from the commercial column and placed in a pipet to minimize loss of material on the column. Monomers were then sealed, refrigerated at 6 °C and stored in the dark before use.

The main photoinitiator in these studies was 2-methyl-1-[4-(methylthio)phenyl]-2-morpholinopropan-1-one (**1**), obtained from Ciba-Geigy and used without purification. Michler's ketone [4,4′-bis(dimethylamino)benzophenone], obtained from Aldrich Chemical Co., was employed occasionally without purification to demonstrate the independence of phenomena from the particular initiator used.

Solutions of typically 0.006% (w/w) of initiator dissolved in monomer were degassed in 5-mm-diameter glass tubes on a vacuum line with a sufficient number of freeze−pump−thaw cycles to reach $<2 \times 10^{-5}$ Torr of pressure. Some control experiments with Michler's ketone were repeated at higher concentrations to achieve better signal levels. The sample tubes were then sealed off under vacuum with a torch. The methyl methacrylate and methyl acrylate monomer samples were prepared similarly, initially with initiator solutions at higher concentrations. Then they were dissolved into poly(methyl methacrylate) (PMMA, 93 300 amu) from Aldrich Chemical Co. to accelerate propagator radical buildup by means of the increased viscosity. The PMMA was shown to be free of detectable EPR signals. Inhibitor removal and sample preparations were carried out under yellow lamp light (GE F40060 Gold).

The samples were irradiated with a 1000-W Hg−Xe arc lamp through a 10-cm H_2O heat filter, a Corning CS-054 310-nm low-pass cutoff filter, and a Corning CS-754 250−390-nm band-pass filter with a beam power incident on the sample of approximately 130 mW. The lamp was outfitted with a mirror and a 5-cm-diameter collector−collimator lens. The filtered light was focused to a beam of 1-cm diameter at the sample in the EPR cavity. All sample preparations and experiments were carried out at room temperature.

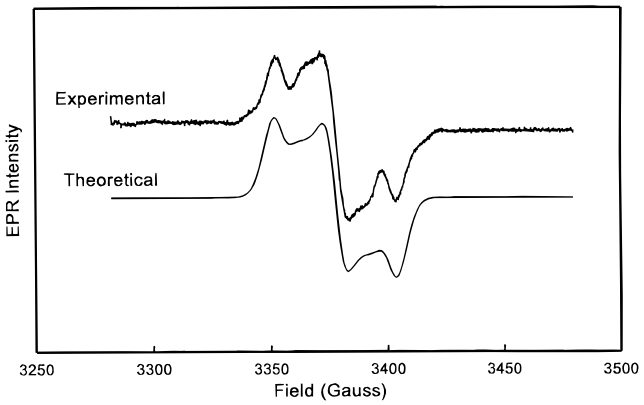

Figure 1. Experimental EPR spectrum of free radicals generated from the polymerization of MA monomer in the presence of PMMA. Also shown is the calculated spectrum obtained from the least-squares fit of the calculated hyperfine lines to the spectrum according to the midchain radical model.

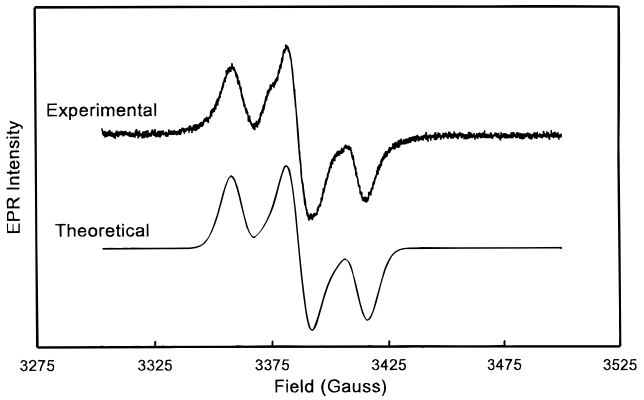

Figure 2. Experimental EPR spectrum of free radicals generated from the polymerization of HDA monomer. Also shown is the calculated spectrum obtained from the least-squares fit of the calculated hyperfine lines to the spectrum according to the midchain radical model.

The CW EPR spectrometer and associated digital data acquisition system have been described recently.[23,24] The pulsed EPR experiments were performed on a Bruker ESP-380 pulsed EPR spectrometer with a dielectrically loaded cylindrical cavity. Spectra analyzed in this paper were usually recorded after irradiation gave numbers of free radicals approaching the long irradiation time limit (usually $>10^3$ s). The two-pulse EPR echo spectra were obtained with $H_1 = 1.4$ G, but were shown in experiments at lower H_1 not to be power-broadened insofar as the present purposes are concerned. Spectra were obtained by digitally recording the echo intensity as a function of magnetic field. Spectra were recorded at systematically varied pulse intervals τ between 150 and 800 ns, the range limited by the spectrometer dead time and the time beyond which the signal level was too low. Some two- and three-pulse echo decays at the narrow lines in the spectra were also examined.

Experimental Results

The CW EPR spectra of the free radicals formed upon irradiation of the initiator **1** in the protonated monofunctional, difunctional, and trifunctional acrylate monomers are shown in Figures 1−3, respectively (together with theoretical fits). Likewise, the monofunctional, difunctional, and trifunctional methacrylate spectra are presented in Figures 4−6, respectively. All of the acrylate-derived spectra show approximately three-line spectra, with some evidence of an additional spectrum interspersed between the lines and in the wings. All of the methacrylate-derived spectra show mainly five-line

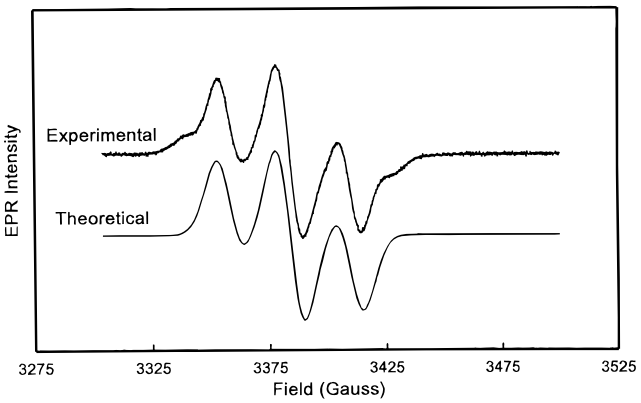

Figure 3. Experimental EPR spectrum of free radicals generated from the polymerization of TMPTA monomer. Also shown is the calculated spectrum obtained from the least-squares fit of the calculated hyperfine lines to the spectrum according to the midchain radical model.

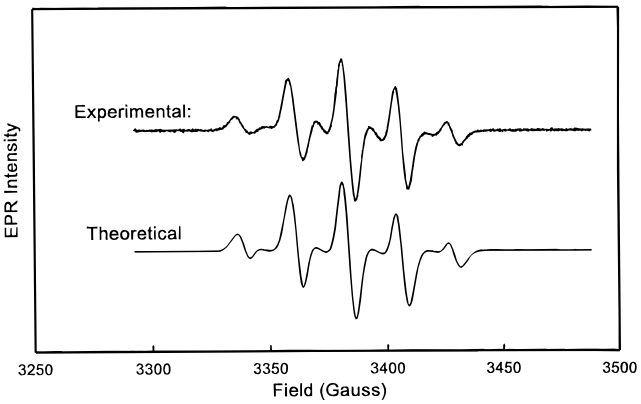

Figure 4. Experimental EPR spectrum of free radicals generated from the polymerization of MMA monomer in the presence of PMMA. Also shown is the calculated spectrum obtained from the least-squares fit of the calculated hyperfine lines to the spectrum according to the orientation distribution model of the propagator radical.

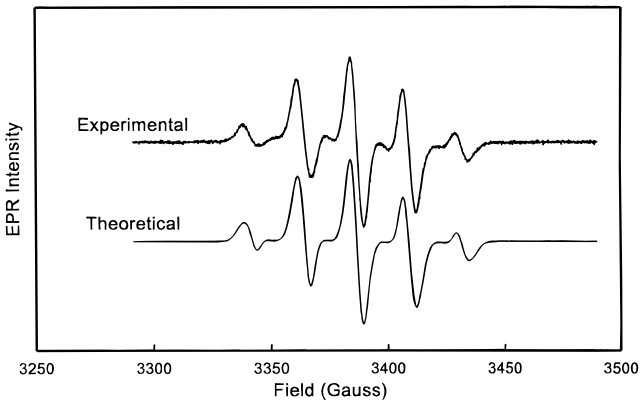

Figure 5. Experimental EPR spectrum of free radicals generated from the polymerization of EGDMA monomer. Also shown is the calculated spectrum obtained from the least-squares fit of the calculated hyperfine lines to the spectrum according to the orientation distribution model of the propagator radical.

spectra, with some evidence of interspersed features. The members of the sets of acrylate-derived and methacrylate-derived spectra display no marked differences between the monofunctional and polyfunctional monomer-derived spectra. The features of the acrylate-derived spectra are markedly broader than those of the methacrylate-derived spectra.

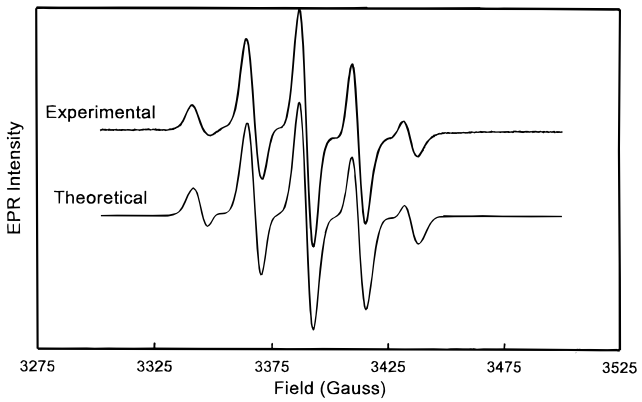

Figure 6. Experimental EPR spectrum of free radicals generated from the polymerization of TMPTMA monomer. Also shown is the calculated spectrum obtained from the least-squares fit of the calculated hyperfine lines to the spectrum according to the orientation distribution model of the propagator radical.

CW EPR spectra from the polymerizations of trifunctional acrylate and methacrylate monomers were obtained with initiator (**1**) and with Michler's ketone. Comparison showed no obvious differences in the spectra other than in the numbers of free radicals accumulated, which was probably a result of the lower initiation efficiency of Michler's ketone. A control experiment was also performed to check for the possible accumulation of free radicals directly from the initiator decomposition or from initiator attack on preexisting polymer chains. For this purpose, **1** was dissolved in a solvent with poly(methyl methacrylate) and then the solution was dried and sealed under vacuum. Irradiation of this sample did give a different free radical EPR spectrum, with intensities several orders of magnitude less than the free radical intensities found with comparable amounts of initiator in the polymerizations.

We have measured the pulsed EPR spectra of polymers from MMA, TMPTA, and TMPTMA at a variety of pulse intervals τ. As expected, the spectrum decays in intensity with increasing τ. However, closer inspection shows that there is a broad underlying spectrum with a somewhat faster decay. The lack of cross-linking in the polymerization of MA monomer, either neat or on PMMA, apparently led to a reduction in the spin−spin or spin−lattice relaxation times and/or the number of free radicals to the point where pulsed EPR spectra were not observed. A shallow three-pulse echo decay modulation was present in the TMPTA experiment, but was not resolved in the other samples.

The CW EPR spectra of free radicals from the polymerizations of MMA-d_2 and MMA-d_3 in PMMA were also obtained. The spectra are shown in Figures 7 and 8. The spectrum from MMA-d_2 is an approximately 1:3:3:1 quartet, as would be expected from three equal methyl group proton hyperfine interactions. The spectrum from MMA-d_3 displays a broad doublet overlaid with the spectrum of a radical, possibly from MMA, present as an isotopic impurity or from unreacted monomer in the added PMMA. The effect of increased viscosity obtained by adding PMMA to monomer is illustrated in Figure 9. EPR intensities of the MA propagating radicals versus time are shown during the irradiations of the initiator **1** in MA in the presence and absence of PMMA.

Analysis of Results

The spectra were fitted by the sets of sharp lines calculated from the model of Sakai and Iwasaki.[12] (In

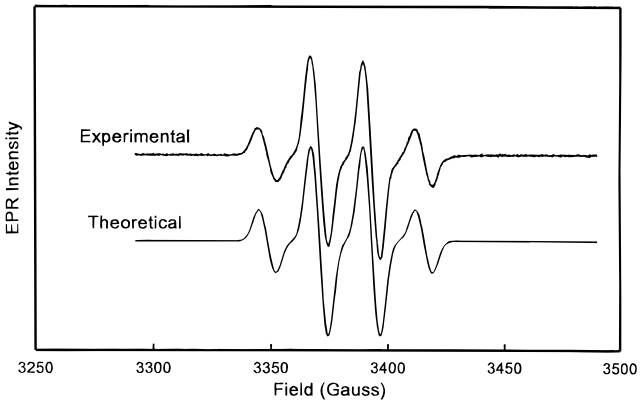

Figure 7. Experimental EPR spectrum of free radicals generated from the polymerization of MMA-d_2 monomer in the presence of PMMA. Also shown is the calculated spectrum obtained from the least-squares fit of the calculated hyperfine lines to the spectrum according to propagator radical model with isotropic, independently varied β-proton hyperfine interactions.

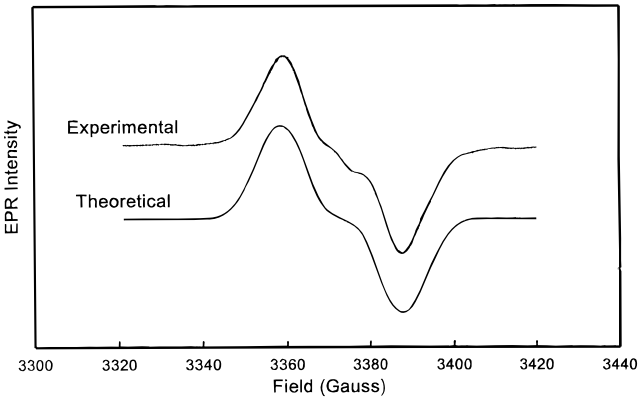

Figure 8. Experimental EPR spectrum of free radicals generated from the polymerization of MMA-d_3 monomer in the presence of PMMA. Also shown is the calculated spectrum obtained from the least-squares fit of the calculated hyperfine lines to the spectrum according to the propagator radical model with isotropic, independently varied β-proton hyperfine interactions.

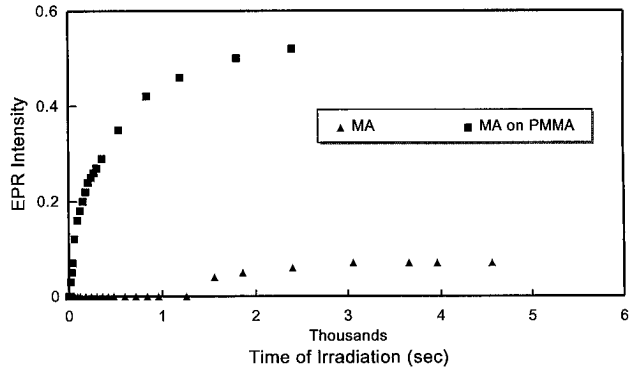

Figure 9. Records of EPR intensity versus time of sample irradiation comparing MA-derived radical intensities in the presence and absence of PMMA.

this model the broadened lines are simply ignored.) In the fits to the methacrylate polymer spectra, the assumption from Sakai and Iwasaki[12] is made (eq 1). The

$$a_{H_{\beta 1}} + a_{H_{\beta 2}} = a_{CH_3} \quad (1)$$

literature values for the α-protons of secondary radicals often have isotropic hyperfine coupling constants similar

Table 1. Results of Fitting the Parameters of the Sakai−Iwasaki-Type Model for the Terminal Radical in the Polymers Derived from the Indicated Acrylate and Methacrylate Monomers[a]

monomer	$\frac{\alpha_{H_{\beta 1}} + \alpha_{H_{\beta 2}}}{g_e\lvert\beta_e\rvert}$ (G)	ΔH (G)
HDA	20.8	11.53
	(0.1)	(0.02)
TMPTA	23.1	11.88
	(0.1)	(0.02)
MMA	22.6	3.82
	(0.1)	(0.01)
EGMDA	22.6	4.36
	(0.1)	(0.01)

[a] A satisfactory fit to the spectrum of the MA polymer was not possible. The standard deviations of the parameters calculated from the fit are given in parentheses.

Table 2. Results of Fitting the Parameters of the Model Assuming Isotropic Proton Hyperfine Interactions of the α- and β-Protons in the Propagator Radicals in Polymers Derived from the Indicated Acrylate and Methacrylate Monomers[a]

monomer	$a_{\beta_H}/g_e\lvert\beta_e\rvert$[b] (G)	$a_{\beta_H}/g_e\lvert\beta_e\rvert$[b] (G)	$a_{H_\alpha}/g_e\lvert\beta_e\rvert$ (G)	$a_{CH_3}/g_e\lvert\beta_e\rvert$[a] (G)	ΔH (G)
HDA	21	5.0	20.9		10.93
	(4)	(0.7)	(0.1)		(0.03)
TMPTA	20.6	6.4	25.8		10.5
	(0.1)	(0.7)	(0.1)		(0.3)
MMA	14.6	8.0		22.3	4.82
	(0.1)	(0.1)		(0.1)	(0.01)
EGDMA	14.7	7.9		22.4	4.87
	(0.1)	(0.1)		(0.1)	(0.01)
TMPTMA	14.8	7.8		22.4	4.99
	(0.1)	(0.1)		(0.1)	(0.01)
MMA-d_2[b]	2.2	1.2		22.3	3.8
	(0.1)	(0.1)		(0.1)	(0.3)
MMA-d_3[c]	14.8	6		3.8	4.6
	(0.1)	(1)		(0.3)	(0.3)

[a] A satisfactory fit to the spectrum of the protonated MA polymer radical was not possible. The standard deviations of the parameters calculated from the fit are given in parentheses. [b] In MMA-d_2 the entries are the deuterium coupling constants $a_{D\beta_1}$ and $a_{D\beta_1}$. [c] In MMA-d_3 the entry is the deuterium coupling constant a_{CD_3}.

to protons in β-methyl groups, $a_{H_a} \approx a_{CH_3}$.[25] The acrylate polymer spectra were fitted while making the corresponding assumption in eq 2. These fits were done

$$\alpha_{H_{\beta 1}} + a_{H_{\beta 2}} = a_{H_\alpha} \quad (2)$$

to assess the possibility that the acrylate polymer radical is the propagator radical **I**. The fits had only two adjustable parameters, $a_{H_{\beta 1}}$ and $a_{H_{\beta 2}}$, and a Gaussian line width parameter, ΔH, besides the trivial spectrum scaling and centering parameters. Any dipolar anisotropy in the hyperfine interactions of the α- and β-protons was neglected. The results of these fits are presented in Table 1. A minimum could not be found in the fit to the spectrum from MA.

To determine how restrictive the conditions imposed by eqs 1 and 2 were, the spectra were fitted with these conditions relaxed. Anisotropy was neglected, as before. The fits had four, nontrivial, adjustable parameters: $a_{H_{\beta 1}}$, $a_{H_{\beta 2}}$, ΔH, and a_{α_H} (in the acrylates) or a_{CH_3} (in the methacrylates). The results of these fits are presented in Table 2. A minimum could not be found in the fit to the spectrum from MA.

In view of the inability of the adapted Sakai−Iwasaki model to fit the MA spectrum, and the suggestion that

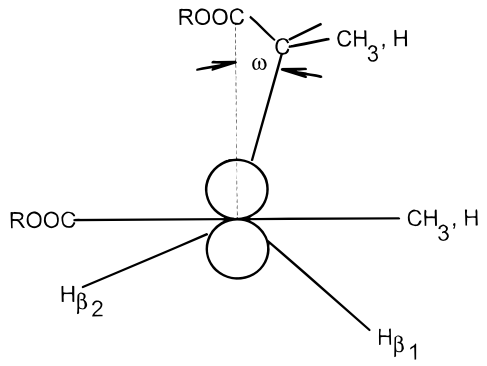

Figure 10. Newman projection of the *p*-orbital of the unpaired electron and the substituent hydrogens and groups on the C center of the (meth)acrylate propagating free radicals.

the MMA spectra exhibit alternating line widths, we turned to the angular distribution model of Best and Kasai.[20] Shown in the Newman projection in Figure 10 is the angle, ω, formed by the projection of the $C_\alpha-C_\beta$ bond on the axis of the p-orbital of the unpaired electron. We consider the possibility of a distribution in the static values of the angles ω and $\omega \pm 2\pi/3$ made by the methylene proton projections on the axis of the p-orbital of the unpaired electron. By ignoring β-proton dipolar interactions, the hyperfine coupling constants given by eqs 3 and 4 are predicted.[26] Equations 3 and 4 are in

$$a_{H_{\beta 1}} = B_0 + B_2 \cos^2(\omega + 2\pi/3) \tag{3}$$

$$a_{H_{\beta 2}} = B_0 + B_2 \cos^2(\omega - 2\pi/3) \tag{4}$$

the form of a well-established empirical relationship that describes the orientation dependence of the isotropic coupling constant of a β-proton in a carbon-centered radical. Values of $B_0/g_e|\beta_e|$ and $B_2/g_e|\beta_e|$ are typically 0−5 and 45 G, respectively. The features in the EPR spectrum for which the quantum numbers of the β-methylene protons are the same will depend on $a_{H_{\beta 1}} + a_{H_{\beta 2}}$. Those for which they are opposite will depend on $a_{H_{\beta 1}} - a_{H_{\beta 2}}$. Equations 5 and 6, obtained by addition and

$$a_{H_{\beta 1}} + a_{H_{\beta 2}} = 2B_0 + B_2 (1 - {}^1/_2 \cos^2 2\omega) \tag{5}$$

$$a_{H_{\beta 1}} - a_{H_{\beta 2}} = -(\sqrt{3}/2)B_2 \sin 2\omega \tag{6}$$

subtraction of eqs 3 and 4, demonstrate that the former features are almost independent of variations in small ω, while the latter will give rise to a distribution of resonance fields that are strongly dependent on the distribution of ω values. That is, the former lines are narrow while the latter are heterogeneously broadened. The Gaussian probability distribution $P(\omega)$ in the ω values of width $\Delta\omega$ around an average angle ω_0, given in eq 7, was employed in the computer simulation and

$$P(\omega) = \frac{\exp\{-[(\omega - \omega_0)/\Delta\omega]^2\}}{\int_{-\infty}^{\infty} \exp\{-[(\omega - \omega_0)/\Delta\omega]^2\}\, d\omega} \tag{7}$$

fit. In practice eqs 3−7 were employed to transform $P(\omega)$ into probability distributions of $a_{H_{\beta 1}} \pm a_{H_{\beta 2}}$ values. The $a_{H_{\beta 1}} \pm a_{H_{\beta 2}}$ intervals in the computation were chosen to be smaller than the spectrum resolution.

We also expected a nonnegligible dipolar interaction from the α-proton in the acrylate polymer propagator radicals. Therefore, the next simulation that we performed also included a powder pattern calculation including the α-proton dipolar interaction over a representative grid of the random orientations of the radical in the magnetic field. The dipolar interactions were assumed to take the values of the α-proton in the glutaconic acid radical,[27] with principal values of −91 MHz when the field **H** is mutually perpendicular to the p-orbital axis and the $C-H_\alpha$ bond, −61 MHz when **H** is parallel to the p-orbital axis, and −29 MHz when **H** is parallel to $C-H_\alpha$. Otherwise forbidden $\Delta m_I = \pm 1$ transitions, made weakly allowed by the presence of the anisotropic α-proton hyperfine interaction, were not included in the calculations of the line shapes. In addition to the four nontrivial parameters in the preceding fit, the Gaussian parameters ω_0 and $\Delta\omega$ were adjusted in this fit, for a total of six parameters. (Actually, in practice, B_0 and B_2 were varied rather than $a_{H_{\beta 1}}$ and $a_{H_{\beta 2}}$.) The results are presented in Table 3.

Finally, to investigate whether the radicals in the acrylate polymers are midchain radicals of structure II, we fitted the spectra with a model that includes two pairs of flanking β-methylene protons. As in the previous fit and according to the Best−Kasai model,[20] we assumed that there are independent distributions in both of the β-methylene group orientations. Two distributions in the two angles ω of the flanking methylene groups were assumed. The distributions were defined and calculated, as described for the previous fit. The parameters ω_{0_1}, ω_{0_2}, $\Delta\omega$, and ΔH were varied in the fit. The results from this minimization are given in Table 4, in which the a_{H_β} values calculated from B_0, B_2, ω_{0_1}, and ω_{0_2} are given for ease of comparison.

To be in a position to assess which models are most appropriate for each spectrum, we collected and compared the mean-squared deviations of each fit in Table 5. Only comparisons between different models for the same type of sample are meaningful. The mean-squared deviations for the spectra of the acrylate polymer radicals have been corrected for deviations in regions of the spectra where there are obvious contributions from the presence of minor amounts of other radicals. The uncertainties have been determined from the mean-squared experimental noise deviations in each spectrum from a best-fit baseline extrapolated to the whole field range of the spectrum.

In the MMA-d_3-derived spectrum $a_{H_{\beta 1}}$, $a_{H_{\beta 2}}$, and a_{CD_3} were varied independently because a satisfactory fit could not be obtained by assuming that

$$a_{H_{\beta 1}} + a_{H_{\beta 2}} = (\gamma_H/\gamma_D) a_{CH_3} \tag{8}$$

Likewise, the MMA-d_3-derived polymer spectrum was fit by variation of $a_{D_{\beta 1}}$, $a_{D_{\beta 2}}$, and a_{CH_3}. The hyperfine coupling constants obtained from these fits are given in Table 2.

We have estimated the T_2 of the sharp- and broad-line parts of the sets of pulsed EPR spectra obtained at various pulse intervals τ. On the basis of the spectrum at long τ, it was assumed that the sharp-line part of the spectrum returns essentially to the baseline between the individual lines in the absence of the broad-line part of the spectrum. The estimated intensity of each sharp-line feature was assumed to be the difference between the peak value and the average of the intensities at the adjacent minima between the peaks. The intensities of the adjacent minima were assumed to be solely due to the broad-line features. Plots such as the one shown

Table 3. Results of Fitting the Parameters of the Methylene Orientation Distribution Model in the Propagator Radical in Polymers Derived from the Indicated Acrylate and Methacrylate Monomers[a]

monomer	$a_{H\beta_1}/g_e\lvert\beta_e\rvert$ (G)	$a_{H\beta_2}/g_e\lvert\beta_e\rvert$ (G)	$a_{CH_3}/g_e\lvert\beta_e\rvert$ (G)	$180\omega_0/\pi$ (deg)	$180\omega_0/\pi$ (deg)	ΔH (G)
HDA	22.0	1.8		17.8	31.3	4.0
	(0.5)	(0.2)		(0.7)	(0.9)	(0.2)
TMPTA	25.8	0.54		23.38	28	4.5
	(0.1)	(0.08)		(0.06)	(1)	(0.2)
MMA	16	4	22.9	10.25	16.4	3.03
	(2)	(2)	(0.1)	(0.06)	(0.2)	(0.03)
EGDMA	17	3	22.8	11.74	18.2	2.79
	(2)	(1)	(0.1)	(0.04)	(0.1)	(0.01)
TMPTMA	17	3.1	22.5	12.03	18.6	3.21
	(2)	(0.9)	(0.1)	(0.04)	(0.1)	(0.02)

[a] Fixed dipolar interaction parameters were used for the acrylate α-proton, as discussed in the text. A satisfactory fit to the spectrum of the MA polymer was not possible. The standard deviations of the parameters calculated from the fit are given in parentheses.

Table 4. Results of Fitting the Parameters of the β-Methylene Protons of the Midchain Radical Model to the Spectra of the Polymers Derived from the Indicated Acrylate Monomers[a]

	methylene 1			methylene 2				
monomer	$a_{H\beta_1}/g_e\lvert\beta_e\rvert$ (G)	$a_{H\beta_2}/g_e\lvert\beta_e\rvert$ (G)	$180\omega_0/\pi$ (deg)	$a_{H\beta_1}/g_e\lvert\beta_e\rvert$ (G)	$a_{H\beta_2}/g_e\lvert\beta_e\rvert$ (G)	$180\omega_0/\pi$ (deg)	$180\Delta\omega/\pi$ (deg)	ΔH (G)
MA	18	4	13	18	4	13	16.5	6.3
	(5)	(3)	(8)	(6)	(3)	(8)	(0.9)	(0.1)
HDA	21	2	16	21	2	16	15.3	5.7
	(5)	(2)	(7)	(5)	(2)	(7)	(0.7)	(0.1)
TMPTA	20.8	2.3	16	24.7	0.8	21.7	16.0	4.0
	(0.8)	(0.4)	(1)	(0.4)	(0.5)	(0.5)	(0.8)	(0.2)

[a] The standard deviations of the parameters calculated from the fit are given in parentheses.

Table 5. Relative Mean-Squared Deviations $\langle\sigma^2\rangle$ of the Fits of the Various Models to the Spectrum of Each Polymer[a]

monomer	Sakai−Iwasaki type (Table 1)	isotropic (Table 2)	propagator angular distribution (Table 3)	midchain angular distribution (Table 4)
MA				25
				(1)
HDA	7.7	7.7	6.7	5.1
	(0.8)	(0.8)	(0.8)	(0.8)
TMPTA	6.7	5.7	2.6	1.0
	(0.2)	(0.2)	(0.2)	(0.2)
MMA	31.6	22.5	8.8	
	(0.4)	(0.4)	(0.4)	
EGDMA	41	37	12	
	(1)	(1)	(1)	
TMPTMA	88.6	75.6	17.9	
	(0.2)	(0.2)	(0.2)	

[a] Standard deviations in the mean squared deviations given in the parentheses are based on the experimental noise in each spectrum. The $\langle\sigma^2\rangle$ for different molecules cannot be compared. The fits whose $\langle\sigma^2\rangle$ are given here are described in detail in the text. The parameters of the fits may be found in Tables 1−4.

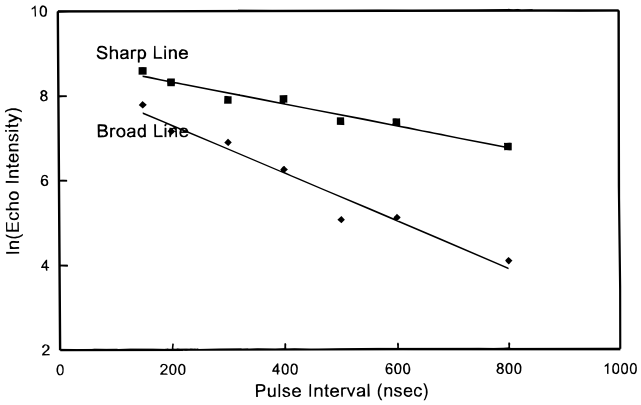

Figure 11. Examples of the logarithmic plots of the echo intensities of the sharp- (top) and broad-line (bottom) parts of the pulsed EPR spectrum of a TMPTMA monomer-derived polymer versus pulse interval τ and the least-squares-fit exponential decays from which spin−spin relaxation times T_2 were obtained.

in Figure 11 for the TMPTMA-derived spectrum were made of the estimated intensities of the sharp-line spectrum at each peak. Similar plots were made of the broad-line spectrum between each pair of sharp-line peaks in the spectrum. The weighted average values of T_2 obtained from the slopes of such plots were calculated. The values are given in Table 6, together with the associated Lorentzian line widths in field units. The Fourier transformation of the three-pulse echo decay[28] of the TMPTMA-derived polymer radical gives two prominent hyperfine interaction frequencies at about 7 and 15 MHz.

Table 6. Spin−Spin Relaxation Times T_2 of the Sharp- and Broad-Line Features in the Pulsed EPR Spectra of the Free Radicals Formed in the Mono- and Trifunctional (Meth)acrylate Polymerizations[a]

monomer	peak type	T_2 (ns)	ΔH (G)
TMPTA	sharp	754 (1.7)	0.1523 (0.0003)
TMPTA	broad	627 (10)	0.181 (0.003)
TMPTMA	sharp	727 (43)	0.156 (0.009)
TMPTMA	broad	367 (30)	0.309 (0.025)
MMA	sharp	1520 (250)	0.075 (0.012)
MMA	broad	806 (18)	0.141 (0.003)
MMA on PMMA[b]	sharp	809 (42)	0.140 (0.007)
MMA on PMMA[b]	broad	607 (29)	0.187 (0.009)

[a] The homogeneous line widths ΔH that correspond to the T_2 are also given. Standard deviations are given in parentheses. [b] MMA is polymerized in the presence of preexisting polymer.

Discussion

Perhaps the most striking result of this study is the inconsistency of the pulsed EPR spin−spin relaxation times with the dynamic β-proton site exchange model of Sakai and Iwasaki.[12] For example, the T_2 time of 369 ± 29 ns observed for the broad-line spectrum is more than an order of magnitude too large for the prediction of 10 ns from the dynamic model. Such a short T_2 time would, in fact, render the broad-line spectrum altogether undetectable in the pulsed EPR spectrometer. Table 6 points out that, rather than having radically different relaxation times, the broad- and narrow-line spectra, in fact, have spin−spin relaxation times on the same order of magnitude. The T_2 of the broad-line part of the spectrum is about a factor of 2 shorter than that of the sharp-line part. Thus, there is an indication of an only slightly greater dynamic contribution to the spin−spin relaxation for the broad-line part of the spectrum than the narrow-line part.

All of the models that we have considered fit the spectra, except MA, with various degrees of success. By and large there are pleasing self-consistencies in the values of $a_{H_{\beta 1}} + a_{H_{\beta 2}}$, a_{CH_3}, and of the corresponding gyromagnetic ratio-scaled deuterium hyperfine interaction constants in the models for the propagator radical in Tables 1−3. The few exceptions appear to belong to the acrylate-derived polymers. The fact that the linewidth parameters (10.5−12.0 G) for the acrylate-derived polymers are over twice as large in the Sakai−Iwasaki-type model in Table 1 and in the isotropic interaction model in Table 2 than in the other fits also seems unreasonable. The latter problem gives the appearance of being ameliorated in the model with anisotropic α-proton dipolar interactions and the distribution of methylene orientations. In summary, the least-squares fits that employ the assumption that the acrylate-derived radical is the propagator radical lack some of the self-consistency that prevails for the methacrylate-derived polymers.

The introduction of an angular distribution of methylene orientations and the introduction of the anisotropic α-proton dipolar interactions give some improvements in the fits, as shown in Table 5, to the HDA- and TMPTA-derived polymer spectra, especially the latter. However, the improvement is relatively small for HDA, and the model does not enable the MA-derived polymer spectrum to be fit at all. Together with the lack of self-consistency in the β-proton parameters of all of these fits with the corresponding methylene parameters in the methacrylate-derived spectra discussed earlier, these results cast strong doubt on whether the acrylate-derived polymer radicals are the propagator radicals. This lends independent spectroscopic evidence to the conclusion of Kloosterboer et al.[4] that the radical observed in a polymer derived from an α-deuterated acrylate monomer cannot be the propagator radical. They observed a spectrum that was essentially identical to a polymer derived from the undeuterated acrylate monomer.[4] They base their conclusion on the assumption that the magnitude of the α-proton interaction is large enough in the propagator radical that an α-deuterated radical would have a substantially different spectrum. The assumption appears to be supported by our estimates of the magnitudes of the α parameters.

The logic of these arguments indicates that the acrylate-derived radical *is not* the propagator radical. However, it lends no direct evidence that the radical is the midchain radical II, attractive as this is on chemical grounds. Best and Kasai[20] addressed this question in part by showing that the spectrum of the radical in a polymer derived from the same monomer used by Kloosterboer et al. can be satisfactorily simulated with a midchain radical model. The midchain radical results presented in Table 4, in comparison with the propagator radical results in Tables 1−3, take the logic a step further. Our results permit us to make quantitative comparisons between the propagator radical I models and the midchain radical II model.

The midchain radical model enables a fit to the MA-derived polymer radical, where a fit was not possible at all with the propagator radical models. The midchain model improves the HDA fit by a small, barely significant amount, as shown in Table 5. The midchain model improves the TMPTA fit by a very significant amount (see Table 5). It should be noted that the additional HDA and TMPTA improvement is no more dramatic than the previous improvement wrought by adding the α-proton anisotropic dipole interaction and the methylene orientation distribution to the propagator radical model. Likewise, the unreasonable acrylate polymer line width, ΔH, in two of the propagator radical models given in Tables 1 and 2 is rectified by the midchain radical model, as shown in Table 4. However, the linewidth parameters, ΔH, in the HDA and TMPTA polymers are even less in the fits with the anisotropic, orientation distribution, propagator radical model. We believe that the ΔH problem in the propagator radical model is replaced by another problem in the propagator radical mode, namely, there are unreasonably large orientation distribution widths $\Delta\omega$ of 28−31°, approaching twice those found in the methacrylate polymers (see Table 3). We believe that this unreasonable adjustment may also account for the fortuitous, dramatic decrease in the mean-squared deviations in these fits. On the balance, we believe that the midchain radical model provides an all-around satisfactory fit to the acrylate data, whereas the propagator model fits are all flawed in one way or another. Thus, we conclude that the radical in the acrylate polymers is the midchain radical II and not the propagator radical I.

As for the methacrylate propagator radical spectra, the isotropic model does give significant improvements in the mean-squared deviations of the fit given in Table 5 over those of the Sakai−Iwasaki model. This is to be expected from the pulsed EPR echo decay measurements, which fail to support the dynamic broadening hypothesis of the Sakai−Iwasaki model. The addition of an angular distribution in the methylene orientation, however, gives dramatic improvements in the mean-squared deviations of the fits given in Table 5. To some extent, the improvement may be wrought at the expense of the reliability of the a_{H_β} values in Table 3, whose standard deviations are significantly larger than those in Table 2 or than the combined values in Table 1. In this connection, we note that one of the β-proton hyperfine coupling constants, as indicated for the TMPTMA polymer by the echo decay modulations, should indeed be in the neighborhood of 15 MHz, in better agreement with the results of the isotropic model in Table 2 than the results of the angular distribution model in Table 3. In spite of the uncertainties introduced into a_{H_β} by the angular distribution model, the dramatic improvements achieved overall in the fits and the tightness and self-consistency with which ω_0 and $\Delta\omega$ in Table 3 are determined provide convincing evidence that an angular distribution does indeed exist.

In fact, a distribution must exist to account for the selective heterogeneous broadening of alternate lines that obviously exists in the methacrylate polymer spectra in Figures 4−6.

According to the results of the least-squares fits in Table 3, there is a high statistical certainty in ω_0 and $\Delta\omega$ in the distributions of methylene orientations in the methacrylate polymer radicals. Apparently, there are relatively small but significant increases in ω_0 and $\Delta\omega$ with greater monomer functionality. This may be the result of the repulsion of the adjacent repeating unit by the COOR group that results from strained cross-link from the COOR group to other polymer chains, resulting in greater ω_0 (see Figure 10). Thus, the increasing monomer cross-linking ability in the order MMA < EGDMA < TMPTMA would result in greater average strain, likewise increasing ω_0. It would also be reasonable to expect the width of the distribution in the strain of the linkages to increase in this order, thereby leading to increases in $\Delta\omega$.

On the other hand, it would not be unreasonable to question the significance of the very small (1−2°) differences in ω_0 and $\Delta\omega$ in Table 3. The data make it very clear that the polymer chain conformations and conformation distributions determine ω_0 and $\Delta\omega$. The relative uniformity in ω_0 and $\Delta\omega$ shows that the degree of cross-linking has relatively little effect on the distribution of propagating radical structures.

The angular distributions of the flanking methylene groups of the midchain radicals in the polyacrylates, determined in the least-squares fits, are given in Table 4. The ω_0 values of both methylenes, which were not constrained to be equal (as were the widths $\Delta\omega$), assumed equal values in the fits to the MA- and HDA-derived radical spectra, but assumed significantly different values in the TMPTA fit. While there appear to be increases in ω_0 with increased monomer functionality, the increases are not statistically significant. The widths $\Delta\omega$ of the distributions also remain constant within experimental error. Where statistically significant, the ω_0 values are larger than their counterparts in the methacrylate propagating radical. Presumably, the COOR group at the midchain radical center is repelled more by the *two* flanking COOR groups than is the COOR group at the methacrylate propagating radical center by the *single* COOR in the preceding monomer unit. Apparently, like the methacrylate propagating radical, increases in acrylate polymer cross-linking have little, if any, effect on the midchain radical's ω_0 or $\Delta\omega$. It is not clear why the TMPTA polymer radical adapts two different ω_0 values.

There is an underlying spectrum or spectra in the radicals found in the acrylate polymerizations (see Figures 1−3). Features appear at the sides of the central peak and also above and below the highest and lowest field extremes in the spectra that are not reproduced by (any of) the simulations. It has also been noted by Bellobono et al.[13] that a broad peak exists in the EPR spectra of acrylate-derived polymers. The spectra have an integrated intensity of about twice that of the three-line spectrum and identical thermal kinetic behavior.[13] While we have not attempted to perform an analysis of residuals in our least-squares fits, the magnitudes of our corrections for the broad background signals are also substantial. Best and Kasai[20] show that the spectrum is consistent with a midchain radical derived from a *gauche,gauche* precursor mixed with a minor amount of midchain radical from a *trans,gauche* or *gauche,gauche* precursor. This would be consistent with the similar chemical kinetic behavior observed for the two radicals by Bellobono et al.,[12] but does not appear to be fully consistent with the magnitudes of the background spectra observed in our study and the study of Bellobono et al.[12]

Conclusions

The time-resolved, pulsed EPR experiments show that the alternating line widths in stable acrylate and methacrylate macroradicals are not due to the motions of the methylene groups adjacent to the free radical center, as proposed by Sakai and Iwasaki.[12] Alternate EPR lines are broadened heterogeneously, not homogeneously, as a consequence of a distribution of static methylene group orientations with respect to the odd electron orbital axis proposed by Best and Kasai.[20] Least-squares fits of relevant models to the EPR spectra also demonstrate the statistical superiority of the heterogeneous broadening model.

We have systematically least-squares-fitted several relevant models to the EPR spectra of the stable radicals in series of monofunctional, difunctional, and trifunctional acrylates and methacrylates. These results independently confirm the conclusion of Kloosterboer et al.[4] that the acrylate polymer radicals are not the propagating free radicals. The results also confirm Best and Kasai's demonstration[20] that the spectrum of the acrylate radical is consistent with a polyacrylate midchain radical formed by hydrogen abstraction at the unstable *gauche,gauche* centers. Our results demontrate that the fits of the midchain radical model to the spectra are statistically superior to the fits of a propagator radical model.

The methylene orientation distributions in both the acrylate midchain radical and the methacrylate propagator radical appear to reflect the *number* of ester groups adjacent to the radical center. However, the orientation distributions are relatively insensitive to the cross-linking potential via the ester.

Acknowledgment. We acknowledge the IBM Corporation, Endicott, NY (under Agreement No. 0035), for financial support of this work and Professor Nicholas J. Turro, Department of Chemistry, Columbia University, for the use of the Bruker pulsed EPR instrument in these experiments. R.C.M. acknowledges the financial support of the Department of Chemistry at the State University of New York at Binghamton and the U. S. Department of Energy. We acknowledge the referees' helpful suggestions.

References and Notes

(1) Fraenkel, G. K.; Hirshon, J. M.; Walling, C. *J. Am. Chem. Soc.* **1954**, *76*, 3606.
(2) Bamford, C. H.; Ingram, D. J. E.; Jenkins A. D.; Symons, M. C. R. *Nature* **1955**, *175*, 894.
(3) Pappas, S. P., Ed. *UV Curing: Science and Technology*; Technology Marketing Corporation: Norwalk, CT, 1978.
(4) Kloosterboer, J. G.; Lijten, G. F. C. M.; Greidenus, F. J. A. M. *Polym. Rep.* **1986**, *27*, 268.
(5) DeForest, W. S. *Photoresist Materials and Processes*; McGraw-Hill: New York, 1975; pp 181−182.
(6) Zhu, S.; Tian, Y.; Hansielec, A. E.; Eaton, D. R. *Polymer* **1990**, *31*, 1726.
(7) Tsukahara, Y.; Tsutsumi, K.; Yamashita, Y.; Shimada, S. *Macromolecules* **1990**, *23*, 5201.
(8) Abraham, R. J.; Melville, H. W.; Ovenall, D. W.; Whiffen, D. H. *Trans. Faraday Soc.* **1958**, *54*, 1133.
(9) Atherton, N. M.; Melville, H.; Whiffen, D. H. *J. Polym. Sci.* **1959**, *34*, 199.

(10) Keah, H. H.; Rae, I. D.; Hawthorne, D. G. *Aust. J. Chem.* **1992**, *45*, 659.
(11) Bamford, C. H.; Bibby, A.; Eastmond, G. C. In *International Symposium on Macromolecular Chemistry*, Prague, 1965; Wichterle, O., Sedlácek, B., Eds.; Interscience: New York, 1967; p 2417 (*J. Polym. Sci. C, 16*).
(12) Sakai,Y.; Iwasaki, M. *J. Polym. Sci. A-1* **1969**, *7*, 1719.
(13) Bellobono, I. R.; Oliva, C.; Morelli, R.; Selli, E.; Ponti, A. *J. Chem. Soc., Faraday Trans.* **1990**, *86*, 3273.
(14) Kuzuya, M.; Noguchi, A.; Ishikawa, M.; Koide, A.; Sawada, K.; Ito, A.; Noda, N. *J. Phys. Chem.* **1991**, *95*, 2398.
(15) Bowden, M. J.; O'Donnell, J. H. *J. Phys. Chem.* **1968**, *72*, 1577.
(16) Smith, P.; Gilman, L. B.; DeLorenzo, R. A. *J. Magn. Reson.* **1973**, *10*, 179.
(17) Horsfield, A.; Morton, J. R.; Whiffen, D. H. *Mol. Phys.* **1961**, *4, 327*, 425.
(18) Liang, R. H.; Tsay, F. D.; Gupta, A. *Macromolecules* **1982**, *15*, 974.
(19) Liang, R. H.; Tsay, F. D.; Gupta, A. *Polym. Mater. Sci. Eng.* **1983**, *49*, 143.
(20) Best, M. E.; Kasai, P. H. *Macromolecules* **1989**, *22*, 2622.
(21) Gilbert, B. C.; Smith, J. R. L.; Milne, E. C.; Whitwood, A. C.; Taylor, P. *J. Chem. Soc., Perkin Trans. 2* **1994**, 1759.
(22) Ichikawa, T.; Yoshida, H. *J. Polym. Sci. A* **1990**, *28*, 1185.
(23) Doetschman, D. C.; Dwyer, D. W.; Trojan, K. *Chem. Phys.* **1989**, *129*, 285.
(24) Das, U.; Doetschman, D. C.; Dwyer, D. W.; Mustafi, M. *Chem. Phys.* **1990**, *143*, 253.
(25) Wertz, J. E.; Bolton, J. R. *Electron Spin Resonance*; *Elementary Theory and Practical Applications*; McGraw-Hill: New York, 1972.
(26) Carrington, A.; McLachlan, A. *Introduction to Magnetic Resonance*; Chapman and Hall: New York, 1979.
(27) Heller, C.; Cole, T. *J. Chem. Phys.* **1962**, *37*, 243.
(28) Mims, W. B. In *Electron Paramagnetic Resonance*; Geschwind, S., Ed., Plenum Press: New York, 1972.

MA951444W